OPEN ACCESS Freely available online

PLOS ONE

Autoproteolysis and Intramolecular Dissociation of *Yersinia* YscU Precedes Secretion of Its C-Terminal Polypeptide $YscU_{CC}$

Stefan Frost[1], Oanh Ho[2], Frédéric H. Login[1], Christoph F. Weise[2], Hans Wolf-Watz[1]*, Magnus Wolf-Watz[2]*

1 Department of Molecular Biology and The Laboratory for Molecular Infection Medicine Sweden (MIMS), Umeå University, Umeå, Sweden, **2** Department of Chemistry, Chemical Biological Center, Umeå University, Umeå, Sweden

Abstract

Type III secretion system mediated secretion and translocation of Yop-effector proteins across the eukaryotic target cell membrane by pathogenic *Yersinia* is highly organized and is dependent on a switching event from secretion of early structural substrates to late effector substrates (Yops). Substrate switching can be mimicked *in vitro* by modulating the calcium levels in the growth medium. YscU that is essential for regulation of this switch undergoes autoproteolysis at a conserved N↑PTH motif, resulting in a 10 kDa C-terminal polypeptide fragment denoted $YscU_{CC}$. Here we show that depletion of calcium induces intramolecular dissociation of $YscU_{CC}$ from YscU followed by secretion of the $YscU_{CC}$ polypeptide. Thus, $YscU_{CC}$ behaved *in vivo* as a Yop protein with respect to secretion properties. Further, destabilized *ysc*U mutants displayed increased rates of dissociation of $YscU_{CC}$ *in vitro* resulting in enhanced Yop secretion *in vivo* at 30°C relative to the wild-type strain.These findings provide strong support to the relevance of $YscU_{CC}$ dissociation for Yop secretion. We propose that $YscU_{CC}$ orchestrates a block in the secretion channel that is eliminated by calcium depletion. Further, the striking homology between different members of the YscU/FlhB family suggests that this protein family possess regulatory functions also in other bacteria using comparable mechanisms.

Citation: Frost S, Ho O, Login FH, Weise CF, Wolf-Watz H, et al. (2012) Autoproteolysis and Intramolecular Dissociation of *Yersinia* YscU Precedes Secretion of Its C-Terminal Polypeptide $YscU_{CC}$. PLoS ONE 7(11): e49349. doi:10.1371/journal.pone.0049349

Editor: Eric Cascales, Centre National de la Recherche Scientifique, Aix-Marseille Université, France

Received June 13, 2012; **Accepted** October 8, 2012; **Published** November 21, 2012

Funding: This research was financially supported by the Swedish Research Council (HWW and MWW), the UCMR Linnaeus Postdoctoral Program (to HWW), the Laboratory of Molecular Infection Medicine Sweden (MIMS, to HWW), and an Umeå University Young Researcher Award (to MWW). The funders had no role in study design, data collection and analysis, decision to publish, or preparation of the manuscript.

Competing Interests: The authors have declared that no competing interests exist.

* E-mail: hans.wolf-watz@molbiol.umu.se (HW-W); magnus.wolf-watz@chem.umu.se (MW-W)

Introduction

In 1952, Hills and Spurr showed that virulent strains of *Yersinia pestis* (*Pasturella pestis*) were unable to grow and divide when incubated at 37°C; instead, they required incubation at 27°C [1]. This phenotype was surprising, because *Y. pestis* causes lethal infections in rodents and humans, which have a body temperature close to 37°C. Moreover, no typical nutritional requirements could explain this phenotype. Later, Kupferberg and Smith demonstrated that addition of 2.5 mM calcium to the growth medium supported growth of *Y. pestis* at 37°C [2]. This unusual requirement for calcium was later shown to be correlated to the massive synthesis and secretion of a number of proteins, called *Yersinia* outer proteins (Yops). This was based on the observation that 2.5 mM calcium in the growth medium blocked Yop secretion, while depletion of calcium induced massive Yop secretion that also results in stop of bacteria proliferation [3,4,5]. Synthesis and secretion of Yops are dependent on a virulence plasmid [6], a common feature of all human pathogenic *Yersinia* (*Y. pestis*, *Y. enterocolitica*, and *Y. pseudotuberculosis*). Yops are synthesized during infection, which indicates their importance in virulence [3]. Yop secretion involves the type III secretion system (T3SS) of *Yersinia*, which is encoded by the same virulence plasmid that carries the *yop* genes. The T3SS is a dedicated secretion system that forms a multi-protein complex of around 25 proteins spanning the inner and outer bacterial membranes [7]. It is built up by a basal body located in the membrane showing high homology with a corresponding structure of the bacterial flagellum. A needle is anchored to the basal body forming hollow tube measuring around 60 to 80 nm in length and 8 nm in external width with an inner diameter of 3 nm [8,9]. It has been postulated that Yops are transferred to the target cell through the needle structure [8]. This model has however been challenged in recent work from our laboratory [10] where we show that bacterial surface localized Yop-effectors can be translocated into the target cell. Hence, translocation can occur via a mechanism that is distinct from the postulated micro-injection model. *Yersinia* employs the T3SS to secrete Yops into the external environment and to translocate Yops into the cytoplasm of eukaryotic target cells [11]. These processes are highly regulated. It has been shown that *Y. pseudotuberculosis* up-regulates *yop* expression after contact with eukaryotic cells, and this requires a functional T3SS [12,13]. Importantly, target cell contact can be mimicked by depleting calcium in the growth medium and simultaneously shifting the temperature from 26°C to 37°C [11]. Modulation of calcium levels in the growth medium has been an invaluable tool for

increasing our understanding of T3SSs in *Yersinia* virulence. Several seminal and general discoveries have been made based on the calcium effect, including T3SS mediated secretion, translocation, and target cell induced expression of effector proteins [12,13,14].

The YscU protein of *Yersinia* is an integral inner-membrane protein with four membrane spanning segments (Figure 1A) and is required for T3SS function. It belongs to a family of proteins (YscU/FlhB class) that is characterized by auto-cleavage at a highly conserved N↑PTH motif (amino acids 263–266) [15]. Autoproteolysis of YscU is required for proper regulation of Yops synthesis and secretion. Furthermore, the Yop synthesis and secretion is lost when the full *ysc*U gene or the N↑PTH coding sequence are deleted, indicating the importance of YscU for T3SS function. Similar phenotypes are observed when point mutations affect cleavage at the N↑PTH motif; this illustrates the importance of cleavage for calcium regulation [16,17,18,19]. Full length YscU (denoted YscU) contains two domains, the transmembrane domain (TM) and a soluble cytoplasmic domain, denoted $YscU_C$ (Figure 1A and Figure 1B). Autoproteolysis of YscU occurs between asparagine 263 and proline 264 at the N↑PTH motif and results in a 10 kDa C-terminal polypeptide fragment, denoted $YscU_{CC}$ that is attached to the remainder of the protein through protein-protein interactions. In context of the cytoplasmic domain, $YscU_C$ (which is used extensively in this article), cleavage generates two fragments; the $YscU_{CC}$ fragment and a 6 kDa N-terminal fragment denoted $YscU_{CN}$ [16,18] (Figure 1A).

Both YscP (FliK) and YscU (FlhB) have been linked to the "substrate specificity switch", first identified by MacNab and coworkers in the flagellum T3SS [15,20]. This switching machinery changes secretion specificity from early hook substrates to late filament substrates as one step in the assembly of the flagellum [21]. It has been suggested that the C-terminal domain of FliK ($FliK_C$) binds to the C-terminal cytosolic domain of FlhB ($FlhB_C$), causing a conformational change in $FlhB_C$ that is required for the switch [20]. An *ysc*P mutant was impaired in switching from the early secretion of needle subunits (YscF) to the late export of Yops [16,22]. This led to a phenotype with unusually long needles unable to secrete Yop proteins, thus YscP is an essential protein for T3SS mediated secretion [16,22,23]. A similar phenotype was observed for the *ysc*U mutant, *N263A*, which highlighted the importance of YscU autoproteolysis in the substrate specificity switch [16]. Interestingly, an *ysc*P null mutant was suppressed by single amino acid substitutions in $YscU_C$, and these suppressor mutants partially restored Yop secretion [17]. This suggested that YscU and YscP interact, and that this interaction was essential for proper control of needle formation and Yop secretion [16]. A direct interaction between the YscU and YscP orthologs, Flik and FlhB has been shown with surface plasmon resonance experiments [24]. In analogy, mutations in the corresponding *ysc*P gene in *Shigella flexneri* (*spa32*) and *Salmonella thypimurium* (*invJ*) [25] also caused defective substrate switching. It has been shown that Spa32 (YscP) and Spa40 (YscU) interact [26,27]. Given the high functional similarity between the T3SSs of different species, it is likely that the substrate specificity switch is regulated by a similar mechanism in different pathogens.

Here, we studied the functional role of YscU in Yop secretion by exploiting the calcium regulation of substrate switching in *Y. pseudotuberculosis*. We combined *in vivo* and *in vitro* methods to examine the steps of YscU autoproteolysis, subsequent dissociation, and secretion of $YscU_{CC}$ and how they affect Yop secretion in *Y. pseudotuberculosis* during growth in calcium depleted media.

Materials and Methods

Bacterial Strains, Plasmids, and Growth Conditions

Bacterial strains and plasmids used in this study are listed in the supporting material ("Table S1"). *Escherichia coli* strains were grown in Luria-Bertani broth (LB) or on Luria agar plates at 37°C. *Y. pseudotuberculosis* was grown at either 26°C or 37°C in Hepes buffered LB or on Luria agar plates (unless specified in the text). Antibiotics were used for selection according to the resistance markers carried by the strains at the following concentrations: kanamycin, 50 μg/ml; chloramphenicol, 25 μg/ml; and carbenicillin, 100 μg/ml. EGTA was added to the media at a final concentration of 5 mM and 20 mM $MgCl_2$ to create calcium depleted conditions.

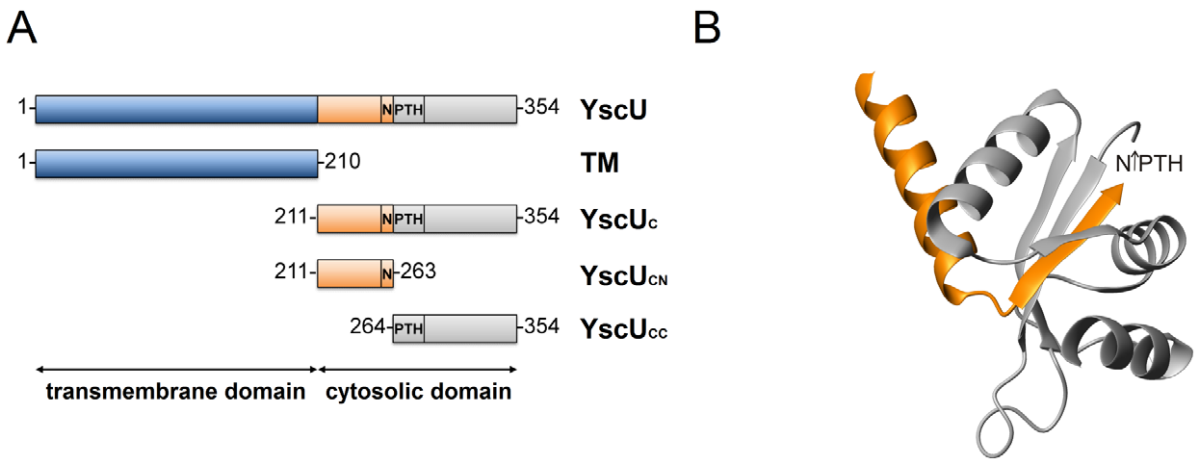

Figure 1. Domain structure of YscU and crystallographic structure of $YscU_C$. (**A**) Schematic domain structure of the integral membrane protein, YscU of *Y. pseudotuberculosis*. The full-length protein contains 354 amino acid residues. The N-terminal 210 residues constitute four transmembrane helices (TM). The cytosolic domain of YscU ($YscU_C$) undergoes autoproteolytic cleavage at the N↑PTH-motif (amino acids 263–266), which leaves an N-terminal cytoplasmic polypeptide, denoted $YscU_{CN}$, and a C-terminal polypeptide, denoted $YscU_{CC}$. (**B**) Ribbon drawing of the cleaved cytosolic domain $YscU_C$ (2JLI.PDB) from *Y. pestis* [39]. $YscU_{CN}$ and $YscU_{CC}$ resulting from cleavage at the N↑PTH motif are colored in orange and grey, respectively.
doi:10.1371/journal.pone.0049349.g001

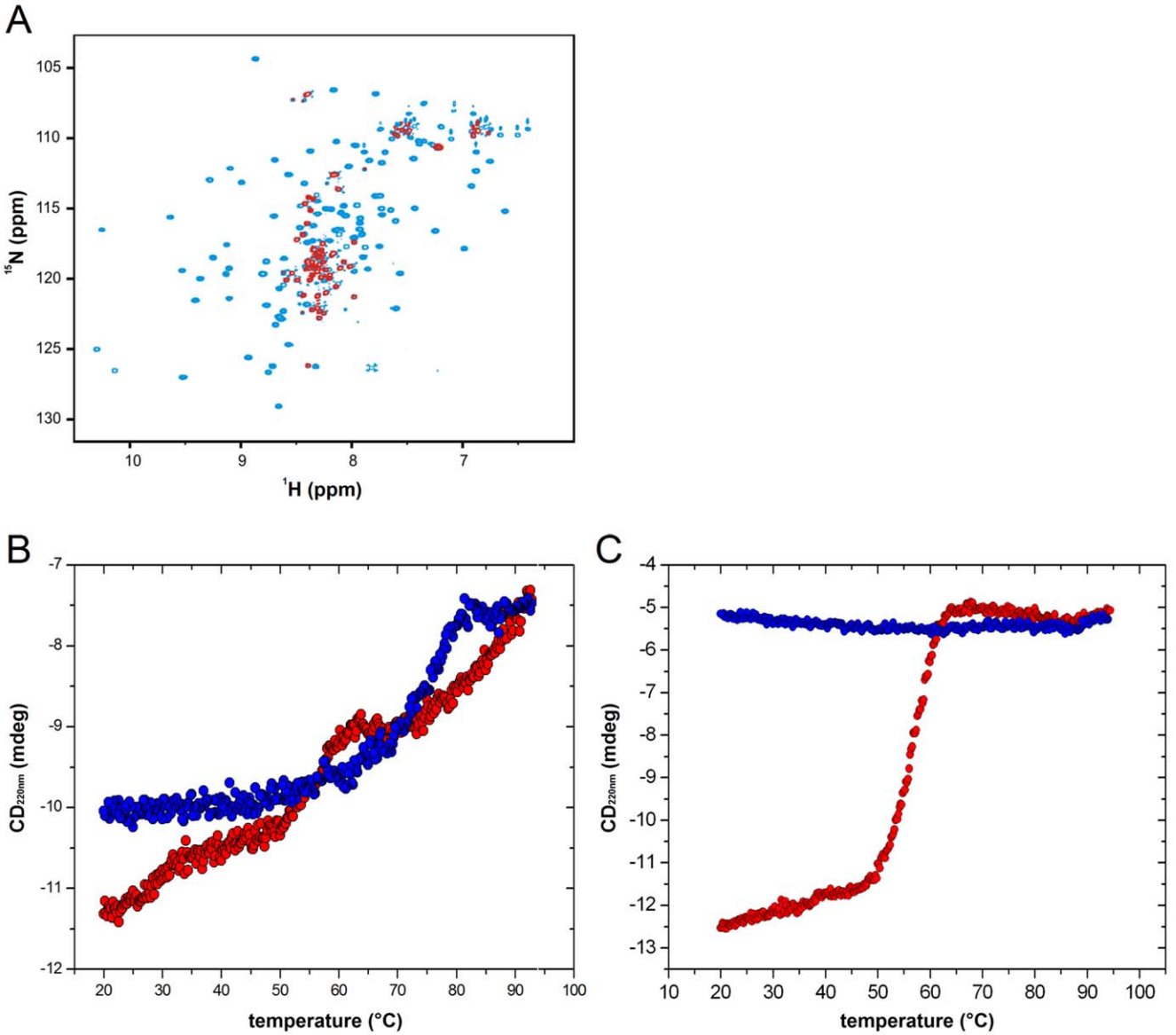

Figure 2. *In vitro* dissociation of YscU$_C$. (**A**) ^{1}H-^{15}N HSQC spectra of YscU$_C$ at 20°C, pH 7.4, before (blue contours) and after (red contours) incubation at 60°C for 10 min. Only resonances that corresponded to YscU$_{CN}$ were visible after the thermal treatment. (**B**) Thermal up- and down-scans of YscU$_C$ at pH 7.4 monitored with CD spectroscopy at 220 nm in the absence of calcium. (**C**) Thermal signatures of P264A, a non-cleavable mutant, at pH 7.4 in the absence of calcium. Up- and down scans of YscU$_C$ and P264A are shown in red and blue circles, respectively.
doi:10.1371/journal.pone.0049349.g002

Yop Secretion Assay

Cultures were started at an absorbance of $OD_{600} = 0.1$ in Hepes buffered LB with the appropriate antibiotics. Bacteria were grown at 26°C for 2 h and shifted to 37°C for 3 h in calcium-supplemented or calcium-depleted conditions (except where specified in the text). Cultures were harvested and centrifuged for 10 min at 4 000×*g*. Aliquots (4.5 ml) of filtrated supernatant were combined with 10% (v/v) trichloroacetic acid (TCA) for protein precipitation. Precipitated proteins were solubilized in SDS-PAGE loading buffer. The pelleted cells were resuspended in an equal volume of LB and lysed with SDS-PAGE loading buffer. Cells and supernatants were loaded at equivalent protein concentrations (according to OD_{600}) and separated by SDS-PAGE. Proteins were either stained with Coomassie R250 or, alternatively, transferred onto a PVDF membrane (GE Healthcare) for immunoblotting. Anti-Yop antibodies were diluted at 1:5 000 and horseradish peroxidase-conjugated anti-rabbit IgG was diluted at 1:10 000 (GE Healthcare). Proteins were detected with a chemiluminescence detection kit (GE Healthcare).

YscU$_{CC}$ Overexpression and Secretion Assay

We grew YPIII/pIB102 bacterial strains, which contained the pBADmycHis B plasmid (Invitrogen) with the *yscU$_{CC}$* expression sequence (see supporting "Material and methods S1"), and control strains contained an empty vector. The growth conditions were as described above, except 0.2% (v/v) of L-arabinose was added after 1 h at 26°C to induce biosynthesis of YscU$_{CC}$. After separation by SDS-PAGE, proteins were stained with Coomassie R250 (Yop secretion) or transferred onto a PVDF membrane (GE Healthcare) for immunoblotting. Anti-YscU$_{CC}$ peptide antibodies were diluted

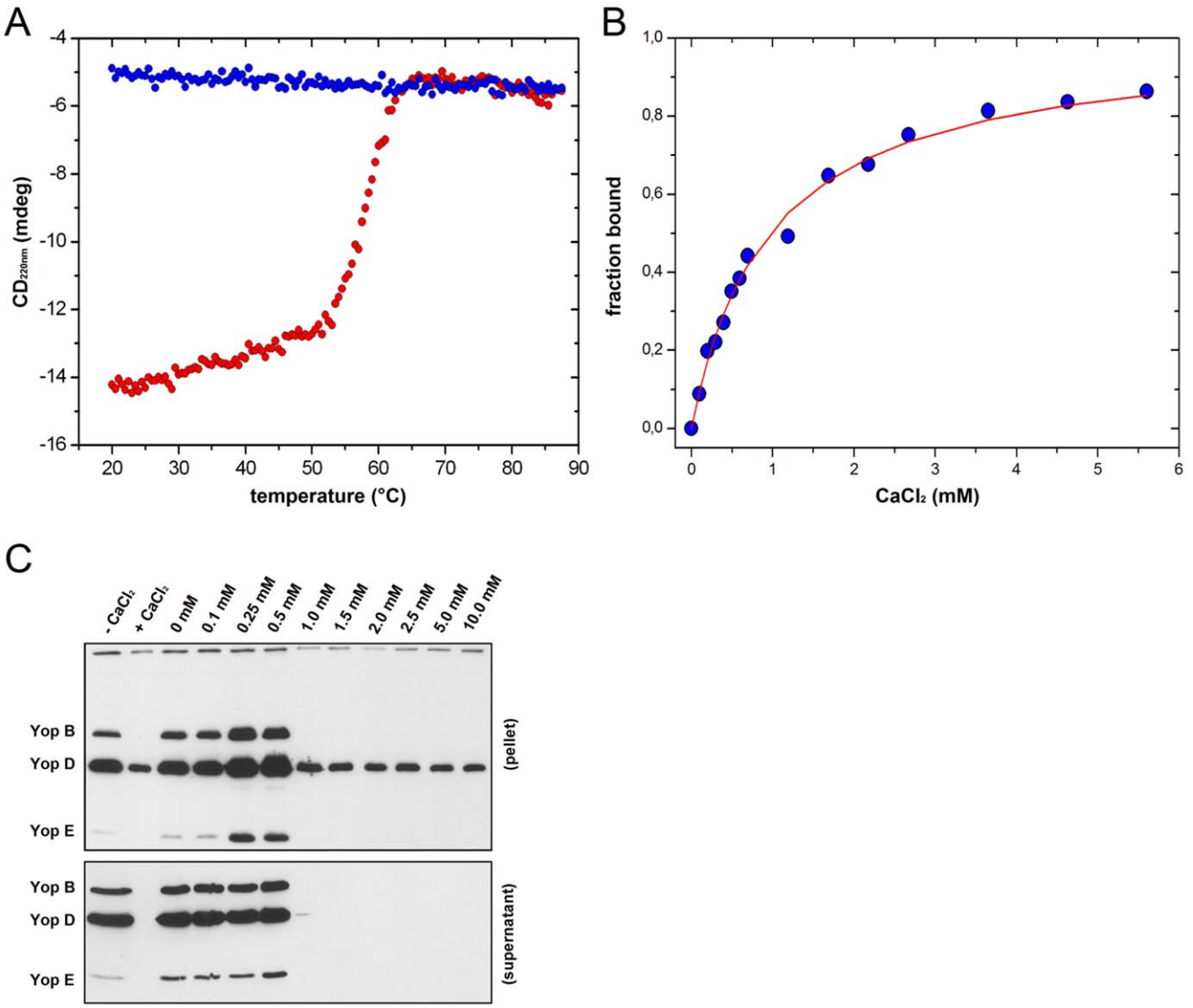

Figure 3. Calcium effects on $YscU_C$ stability and Yop secretion. (**A**) Thermal up- and down-scans of $YscU_C$ at pH 7.4 monitored with CD spectroscopy at 220 nm in the presence of 2.5 mM calcium. Up- and down scans of $YscU_C$ are shown in red and blue circles, respectively. (**B**) Titration of calcium to $YscU_C$ monitored with CD spectroscopy at 220 nm. The calcium binding isotherm to $YscU_C$ was fit to a one-site binding model (red line). The resulting K_d was 800 μM. (**C**) Western Blot analysis of YopB, YopD, and YopE in wild-type *Y. pseudotuberculosis*. The bacteria were grown for 2 h at 26°C and shifted to 37°C for 3 h (temperature shift for induction of Yop secretion) with varying concentrations of free calcium. "Pellet" indicates intracellular proteins; "supernatant" denotes secreted proteins. The LB growth medium was initially supplemented with 1 mM EGTA to complex residual calcium content (approximately 500 μM); thereafter, calcium was added to set the indicated concentrations of free calcium.
doi:10.1371/journal.pone.0049349.g003

at 1:5 000 [16] and horseradish peroxidase-conjugated anti-rabbit IgG was diluted at 1:10 000 (GE Healthcare). Proteins were detected with a chemiluminescence detection kit (GE Healthcare).

GST-pulldown Assay

We purified GST-$YscU_C$-His_6 and GST-A268F-His_6 proteins in 2 steps, by combining GST- and Ni-NTA affinity chromatography. Purified proteins (80 μM) were incubated in 25 mM Tris, pH 7.4, 1 mM EDTA, and 150 mM NaCl at 37°C and 30°C. At different time points, 250 μl samples were taken, centrifuged to remove aggregates (15 min, 16 000×*g* at 4°C), and loaded on GST-SpinTrap™ columns (GE Healthcare). Columns were washed twice with 25 mM Tris, pH 7.4, 150 mM NaCl buffer, and eluted twice by adding 20 mM GSH solution, pH 8.0. Eluted samples were mixed with SDS-sample buffer and boiled. Proteins were subsequently separated and visualized with 4–12% Bis-Tris Gel SDS-PAGE (Invitrogen).

Protein Purification of $YscU_C$ Variants

All $YscU_C$ constructs were cloned as GST fusion with a cleavage site for PreScission Protease between the GST domain and $YscU_C$ (see supporting "Material and methods S2"). After transformation into *E. coli* BL21 (DE3) pLysS the protein synthesis was induced with IPTG and performed overnight at 30°C in LB medium containing carbenicillin and chloramphenicol. The bacterial cells were harvested by centrifugation at 5 000 rpm at 4°C and stored at −80°C until use. The protein purification of $YscU_C$ variants was performed with an ÄKTA purifier system (GE Healthcare). The bacterial pellet was resuspended in 50 mM Tris pH 7.4 and 2 mM DTT, and cells were disrupted by sonication.

Table 1. Dissociation temperatures of $YscU_C$ in presence of different divalent cations and *in vitro* binding affinities.

	$CaCl_2$	$BaCl_2$	$SrCl_2$	$MgCl_2$
Dissociation temperature, T_{diss}				
T_{diss} (°C)	58.5±0.8	57.1±0.3	55.8±0.1	57.9±0.1
Dissociation constant, K_d				
K_d (μM)	800±40	900±140	840±100	130±10

CD spectroscopy at 220 nm was used to monitor thermal up- and down-scans of $YscU_C$ in presence of different divalent cations at a scan rate of 1°C/min to determine dissociation temperatures (T_{diss}, compare Figure 3A). To measure the binding isotherms (K_d) of different divalent cations towards $YscU_C$ (compare Figure 3B) titrations monitored with CD spectroscopy at 220 nm were performed.

doi:10.1371/journal.pone.0049349.t001

The lysate was clarified by centrifugation at 15 000 rpm and 4°C, and the supernatant passed through a 0.45 μm syringe filter (Corning). The lysate, containing the soluble GST fusion protein, was loaded on a 5 mL GSTrap FF column (GE Healthcare) and eluted with 20 mM GSH solution at pH 8.0. Fractions with the fusion protein were pooled, dialyzed at 4°C against cleavage buffer (50 mM Tris pH 7.4, 150 mM NaCl, 1 mM EDTA, 1 mM DTT). The GST protein was cleaved from the target protein by adding PreScission Protease (GE Healthcare). To remove GST and non-cleaved GST-fusion protein the solution was passed through a Glutathione Sepharose 4B column. The flowthrough with $YscU_C$, was subjected to cation exchange chromatography (5 ml SP Sepharose, GE Healthcare). All eluted fractions with $YscU_C$ were pooled, concentrated with Amicon Ultra-15 Centrifugal Filter Units (Millipore, Billerica, MA), and polished with size-exclusion chromatography (HiPrep 26/60 Sephacryl S-100HR, GE Healthcare) in phosphate buffered saline at pH 7.4. Fractions with $YscU_C$ were pooled stored as 100 μM stock at 20°C until use.

Analytical Size Exclusion Chromatography

Protein samples ($YscU_{CC}$) were applied to a Superose 6 10/300 GL column (GE Healthcare) and size-exclusion chromatography (SEC) was performed with a flow rate of 0.5 ml/min in phosphate buffered saline at pH 7.4. Protein elution was followed by monitoring the UV absorption at 260 nm, 280 nm, and 220 nm. All samples with signal peaks at 280 nm were analyzed by SDS-PAGE. Prior to analytical SEC, the column was calibrated with a gel filtration protein standard (Bio-Rad).

NMR Spectroscopy

NMR experiments were performed on a Bruker DRX 600 MHz spectrometer equipped with a 5-mm triple resonance z-gradient cryoprobe. Temperature calibration was conducted with a home-made probe, inserted into the sample compartment of the cryoprobe. The NMR samples contained unlabeled, ^{15}N-labeled, or $^{15}N/^{13}C$ enriched protein in a buffer consisting of 10% $^2H_20$ (v/v), 50 mM NaCl, and 30 mM phosphate buffer at pH 7.4. Backbone $YscU_C$ resonance assignments were accomplished with triple resonance experiments, HNCA [28], HNCOCA, HNCACB [29], and CBCACONH [28], supplemented with a ^{15}N NOESY-HSQC experiment. Chemical shift perturbations were calculated according to: $\Delta\omega = 0.2 \cdot |\Delta^{15}N| + |\Delta^{1}H|$ (ppm).

The time series of one-dimensional ^1H NMR spectra to probe dissociation were acquired with a pulse program from the Bruker library, which incorporated excitation sculpting for water suppression. For each spectrum, 64 scans were accumulated with a relaxation recovery delay of 2 s between scans. For each protein, time series were acquired at 30°C and 37°C. To quantify dissociation kinetics, we integrated the methyl group resonances in the 0.2 to 0.4 ppm spectral region. Each time course of the NMR signal was fit with a single exponential decay function of the form: $I = I_0 \exp^{(-t/\tau diss)} + A$, where τ_{diss} was the lifetime of the decay, and A was a baseline offset. NMR data was processed with NMRPipe [30] and visualized in ANSIG for Windows [31].

Circular Dichroism

Circular dichroism (CD) spectra were recorded on a Jasco J-810 spectropolarimeter, equipped with a Peltier element for temperature control and a 0.1 cm quartz cuvette. The proteins were measured at 10 μM in a buffer of 10-fold diluted phosphate buffered saline at pH 7.4. For all experiments with calcium, different buffers were used (phosphate, MOPS, and Pipes) to exclude possible calcium precipitation effects. Thermal dissociation experiments were performed by monitoring the CD signal at 220 nm as a function of temperature. All thermal profiles were acquired in the interval of 20°C to 90°C. The thermal scan rate was varied from 0.5 to 2°C/min, without any significant change in protein behavior; we selected 1°C/min as the standard condition in this study for CD spectroscopy-based temperature perturbation experiments. The inflection point for dissociation, T_{diss}, was quantified by fitting thermal curves with a two-state equation [32]. Calcium binding affinity was quantified by fitting a one-site binding model to the CD data.

Results

Dissociation of $YscU_{CC}$ from $YscU_{CN}$

We recently published results showing that specific *ysc*U mutants (*N263A* and *P264A*), defective in autoproteolysis, were impaired in their ability to secrete Yops into the culture supernatant at wild-type levels [16]. These mutations strongly reduced the autoproteolytic activity of the YscU protein. Especially the *ysc*U mutant *P264A* was severely suppressed in autoproteolysis leading to an almost complete inhibition of Yop secretion [16]. These results and earlier findings showing that deletion of the autoproteolytic cleavage motif NPTH leads to a complete loss of Yop secretion indicated that the cleavage of YscU is required for Yop secretion [18]. Here, we decided to study YscU in more detail. Because YscU is an integral inner-membrane protein, we produced a polypeptide that comprised the cytosolic segment of YscU including the motif for autoproteolytic cleavage ($YscU_C$; Figure 1A and Figure 1B) for *in vitro* studies. For detailed investigation of conformational changes in $YscU_C$ we have used the spectroscopic methods nuclear magnetic resonance (NMR) and circular dichroism (CD).

It was previously proposed that the $YscU_{CC}$ polypeptide dissociates from the remaining, membrane-anchored segment of YscU to allow Yop secretion [16]. To test this hypothesis, we developed biophysical NMR and CD based protocols for the quantification of $YscU_{CC}$ dissociation from $YscU_{CN}$ *in vitro*. The high quality, ^1H-^{15}N HSQC spectrum of $YscU_C$ at 20°C (Figure 2A, blue contours) and the chemical shift dispersion showed that $YscU_C$ was a folded protein under the experimental conditions. We assigned 91% of the non-proline backbone resonances in our protein construct that contained residues 211–354. In the $YscU_C$ crystal structure (2JLI.PDB) the N-terminal residues 241–255 are in a helical conformation. The helix protrudes into solution and the first residue that makes contact

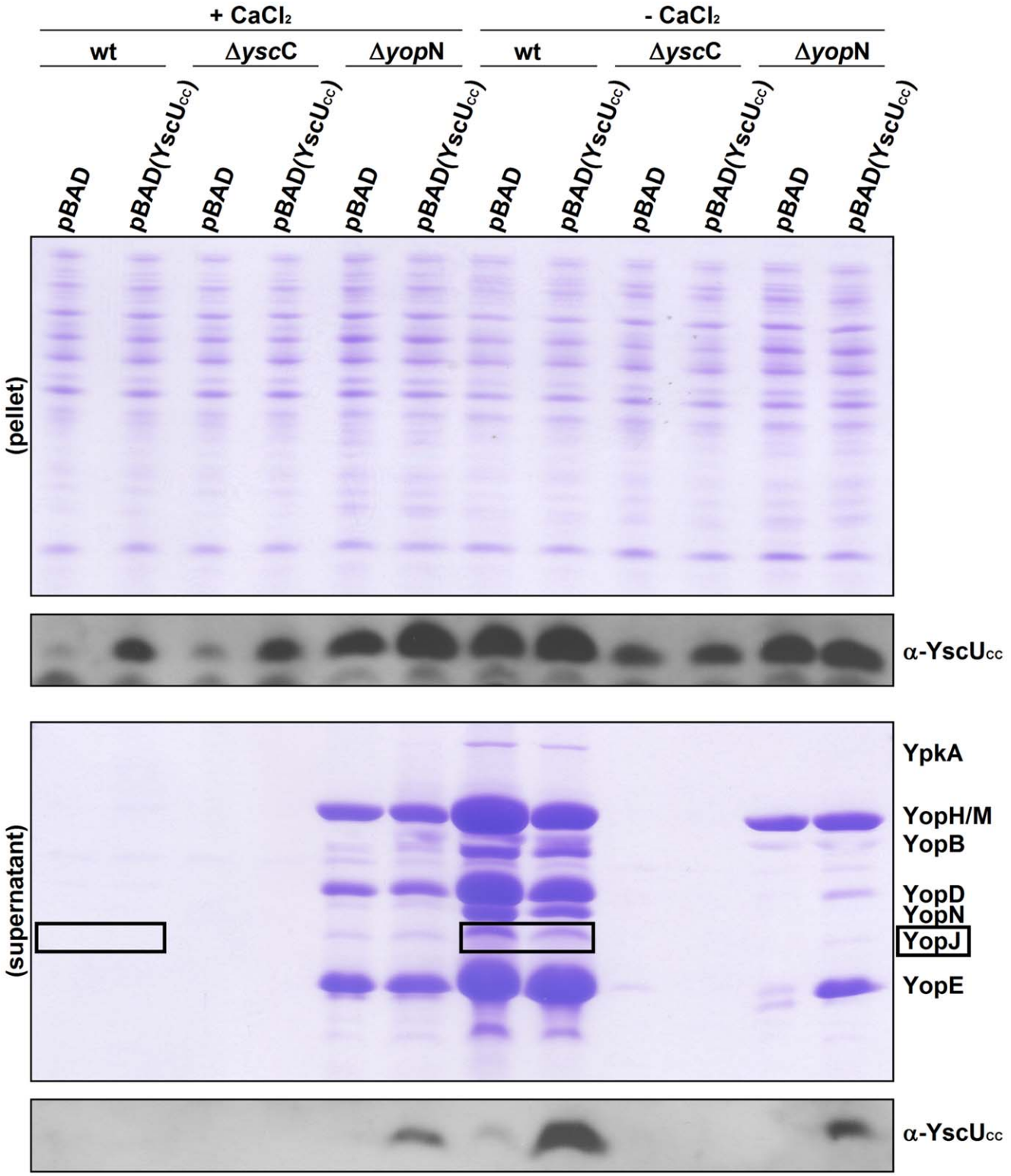

Figure 4. *In vivo* dissociation and secretion of $YscU_{CC}$ in different *Yersinia* strains. Calcium dependent regulation of Yop and $YscU_{CC}$ secretion in wild-type *Y. pseudotuberculosis*, in a Δ*ysc*C mutant and Δ*ysc*N mutant strain without and with *in trans* complementation of $YscU_{CC}$. Bacteria transformed with empty pBADmycHis B (pBAD), or pBAD with one additional $yscU_{CC}$ copy (pBAD($YscU_{CC}$)), were grown for 2 h at 26°C and 3 h at 37°C in calcium depleted (−) or calcium supplemented (+) medium. The expression of $yscU_{CC}$ was induced by addition of arabinose. Yop secretion is coupled to the secretion of $YscU_{CC}$ in all analysed *Yersinia* strains and required a functional T3SS. Secreted Yops visualized on Coomassie stained PAGE gels; $YscU_{CC}$ visualized on immunoblots with anti-$YscU_{CC}$ peptide antibodies. ''pellet'' indicates intracellular proteins; ''supernatant'' denotes secreted proteins. The YopJ protein (black box) was subjected to densitometric analysis for quantification of secretion levels (see Table 2).
doi:10.1371/journal.pone.0049349.g004

Table 2. Comparative densitometric analysis of pH and calcium-dependent Yops secretion in *Y. pseudotuberculosis*.

condition	observed growth attenuation	observed Yop secretion	secretion efficiency (%)
pBAD, $+Ca^{2+}$	no	no	0
pBAD/$YscU_{CC}$), $+Ca^{2+}$	no	no	0
pBAD, $-Ca^{2+}$	yes (+++)	yes (+++)	99
pBAD/$YscU_{CC}$), $-Ca^{2+a}$	yes (+++)	yes (+++)	100
pH 6.0	yes (+)	yes (+)	1
pH 6.5	yes (++)	yes (++)	32
pH 7.0	yes (+++)	yes (+++)	75
pH 7.5[b]	yes (+++)	yes (+++)	100

To compare and quantify the Yop secretion efficiency in wild-type *Y. pseudotuberculosis* under different conditions, Coomassie stained Yop secretion profiles were subjected to densitometric analysis with Multi Gauge software (Fuji Film). The protein YopJ (boxed in Figure 4 and Figure 5E) was selected for quantitative analysis. Growth kinetics in media with different pH's (Figure S4B) showed attenuation of bacterial growth directly linked to the observed Yop secretion efficiency.
[a]secretion efficiency was set to 100%;
[b]secretion efficiency at pH 7.5 was set to 100%.
doi:10.1371/journal.pone.0049349.t002

with the remainder of the protein is residue number 250. In solution the first helical residue that we could identify based on NOE contacts was residue 251, and the assigned preceding residues are adopting an unstructured and flexible conformation as inferred from high signal intensities and narrow chemical shift dispersion. After incubation at 60°C for 10 min, the NMR spectrum of $YscU_C$ at 20°C showed a dramatic perturbation (Figure 2A, red contours); only resonances that corresponded to the $YscU_{CN}$ polypeptide were visible. The narrow chemical shift dispersion and high peak intensities of the $YscU_{CN}$ resonances showed that the polypeptide adopted an unfolded conformation also after dissociation from $YscU_{CC}$. The absence of signals that corresponded to the $YscU_{CC}$ polypeptide was due to the formation of aggregated particles too large for detection with NMR spectroscopy (see supporting material, "Results S1").

The NMR experiments showed that $YscU_{CC}$ dissociation from $YscU_{CN}$ was triggered by subjecting $YscU_C$ to thermal perturbation, and that dissociation was an irreversible process. The irreversibility provided a tool for quantifying dissociation kinetics (discussed below). To obtain an accurate value of the dissociation temperature (T_{diss}), we observed $YscU_C$ dissociation by subjecting the protein to a thermal cycle, and we followed this event with CD at 220 nm. The CD signal at 220 nm contains contributions from both alpha helical and β-strand secondary structures [33]. Thus, because $YscU_C$ contains, both alpha helices and β-strands, 220 nm was a suitable wavelength for following changes in the $YscU_C$ structure (Figure 1B). The thermogram of $YscU_C$ (Figure 2B) was composed of two distinct transitions (55°C and 77°C), and the overall thermal response was not reversible, as the CD signal did not reach its initial value after a complete thermal cycle (see supporting material, "Results S2"). The transition at 55°C corresponded to the dissociation of $YscU_C$; this was in good agreement with the NMR results that showed an upper limit of T_{diss} equal to 60°C. The high temperature transition (77°C) was reversible, but with distinct signs of hysteresis (Figure S1). Because this transition was not relevant in the context of dissociation, we did not study it further. Of note, because dissociation is an irreversible process, T_{diss} is scan-rate dependent. Therefore, all CD spectroscopy-based temperature perturbation experiments were conducted at a fixed scan rate of 1°C/min.

To address the questions whether the dissociation of $YscU_C$ might have biological relevance we subjected the non-cleavable $YscU_C$ mutant P264A to a thermal denaturation. The thermal signature of P264A was dramatically perturbed compared to the wild-type, and the thermogram displayed one irreversible transition at 55°C (Figure 2C). To investigate the biological relevance further, we asked whether calcium might affect the $YscU_C$ dissociation *in vitro*. The thermogram in the presence of calcium was remarkably similar to that of the non-cleavable variant P264A in the absence of calcium (Figure 3A). Hence, calcium mimicked the effect of a mutation that suppressed the $YscU_C$ auto-processing activity. P264A contained one polypeptide chain that could not dissociate; thus, the data suggested that calcium prevented dissociation of $YscU_{CC}$ from the $YscU_{CN}$ polypeptide.

Next we investigated the ability of $YscU_C$ to bind calcium *in vitro* and compared it to the calcium concentration needed to block the Yop secretion *in vivo*. The CD signal at 220 nm indicated the $YscU_C$ binds calcium with a dissociation constant (K_d) of 800 μM, assuming a one-site binding model (Figure 3B). To benchmark the K_d value of calcium against the calcium concentration required for inhibition of the *Yersinia* T3SS *in vivo*, we analyzed Yop secretion and expression at different calcium levels in the growth medium. The T3SS was down regulated at calcium concentrations between 0.5 to 1 mM (Figure 3C). Hence, the *in vitro* K_d value for calcium interaction with $YscU_C$ (800 μM) was well in the concentration interval that inhibited Yop secretion *in vivo*. Comparative analysis with different divalent cations revealed no exclusive specificity of $YscU_C$ towards calcium. Different alkaline earth metals, Mg^{2+}, Ca^{2+}, Sr^{2+} and Ba^{2+} showed comparable effects *in vitro* on $YscU_C$ interaction and dissociation (Table 1). It was not surprising that Ba^{2+} and Sr^{2+} showed a similar effect as Ca^{2+} since these ions have been shown to effect Yop secretion similarly to Ca^{2+} [34]. On the other hand Mg^{2+} has no effect on Yop secretion suggesting that the *in vivo* regulation of calcium controlled secretion is dependent on additional factors. This promiscuous metal binding property of $YscU_C$ is consistent with the absence of any known calcium binding motif in $YscU_C$. In accordance we observed with NMR spectroscopy that calcium binding is mediated through a large set of residues confined to the $YscU_{CC}$ polypeptide (Figure S2).

Nevertheless the *in vitro* data clearly showed that $YscU_C$ was poised for dissociation into $YscU_{CN}$ and $YscU_{CC}$ fragments, and that this event can be inhibited by calcium and other divalent cations. Thus we wondered whether the dissociation of $YscU_C$ could be monitored directly in *Yersinia*, and whether it can be linked to T3SS regulated Yop secretion. To test this idea, we first probed for the presence of $YscU_{CC}$ in the culture supernatants

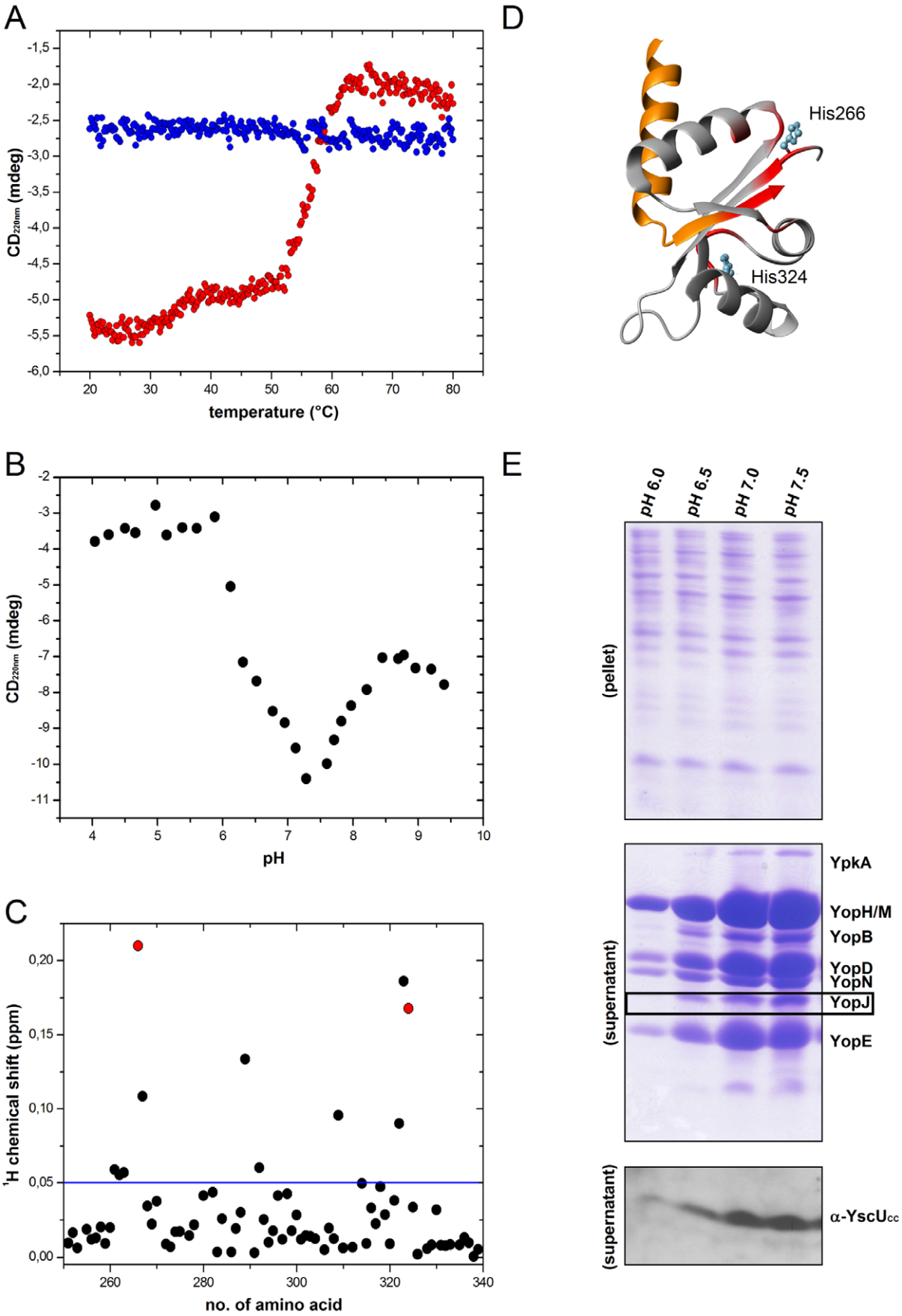
A
CD220nm (mdeg)
temperature (°C)
B
CD220nm (mdeg)
pH
C
1H chemical shift (ppm)
no. of amino acid
D
His266
His324
E
pH 6.0
pH 6.5
pH 7.0
pH 7.5
(pellet)
(supernatant)
YpkA
YopH/M
YopB
YopD
YopN
YopJ
YopE
(supernatant)
α-YscUcc

Figure 5. pH-dependencies of $YscU_C$ dissociation *in vitro* and Yop/$YscU_{CC}$ secretion *in vivo*. (**A**) Thermal up- and down-scans of $YscU_C$ at pH 6.0, monitored with CD spectroscopy at 220 nm in the absence of calcium. The thermal signature of $YscU_C$ displayed one large-amplitude transition at 55°C. Up- and down scans of $YscU_C$ are shown in red and blue circles, respectively. (**B**) The pH-dependency of the $YscU_C$ monitored with CD spectroscopy at 220 nm. (**C**) Chemical shift perturbations of $YscU_C$ quantified from ^1H-^{15}N HSQC spectra, in response to a pH-shift from 7.4 to 6.0, displayed against the primary sequence. The blue line indicates the threshold value (0.05 ppm) used in Figure 5D. The chemical shift perturbation of the two histidines at positions 266 and 324 are shown in red. (**D**) Structural distributions of residues that show significant chemical shift perturbations in response to a pH-shift from 7.4 to 6.0 are shown in red on the $YscU_C$ structure (2JLI.PDB). The $YscU_{CN}$ and $YscU_{CC}$ fragments are colored orange and gray, respectively. The two histidine residues (266 and 324) in the folded part of $YscU_C$ are indicated. (**E**) Coomassie stained gels show Yop secretion under different pH conditions. (top panel) "pellet" indicates intracellular proteins; (middle panel) "supernatant" denotes secreted proteins. The YopJ protein (black box) was subjected to densitometric analysis for quantification of secretion levels (see Table 2). (bottom panel) The pH-dependency of $YscU_{CC}$ secretion was visualized on immunoblots with anti-$YscU_{CC}$ peptide antibodies.
doi:10.1371/journal.pone.0049349.g005

after incubating the wild-type *Y. pseudotuberculosis* strain at 37°C in the absence or presence of 2.5 mM calcium. Remarkably, $YscU_{CC}$ was found in the culture supernatant from the calcium depleted cultures, and no $YscU_{CC}$ was found in cultures with 2.5 mM calcium (Figure 4). To explore this finding further, the gene for the $YscU_{CC}$ polypeptide (amino acids 264 to 354 of YscU) was cloned into the pBAD vector under the control of an inducible *ara*C promoter. This allowed the *in trans* overexpression of *yscU*$_{CC}$ in *Y. pseudotuberculosis*. After promoter induction, the levels of secreted $YscU_{CC}$ were analyzed in cultures grown with or without calcium. We found that induction of *yscU*$_{CC}$ expression caused increased secretion of $YscU_{CC}$ into the culture supernatant when compared to the wild-type levels secreted by a strain that contained the control vector. Further, secretion of $YscU_{CC}$ was blocked in the presence of 2.5 mM calcium in the medium. To investigate the requirement of a functional T3SS for $YscU_{CC}$ secretion we analyzed the secretion behavior of a *Y. pseudotuberculosis* Δ*ysc*C null mutant. In absence of YscC no secretion of either Yops or $YscU_{CC}$ was observed (Figure 4) showing that secretion of $YscU_{CC}$ is dependent on a functional T3SS. To link our *in vitro* findings of $YscU_C$ and calcium directly to *in vivo* events we analyzed the secretion behavior of a Δ*yop*N mutant that has lost its calcium regulation and secretes Yops in presence and absence of calcium in similar amounts [35]. It was found that the Δ*yop*N mutant secreted $YscU_{CC}$ independently of the calcium concentration. Thus, $YscU_{CC}$ was secreted from the Δ*yop*N mutant in the presence of calcium showing a similar secretion profile as the Yop substrates (Figure 4).

In conclusion, $YscU_{CC}$ showed a secretion pattern similar to that of Yops. This suggested that $YscU_{CC}$ constituted a novel substrate of the T3SS in *Yersinia*. Furthermore, the fact that $YscU_{CC}$ was secreted in the wild-type strain demonstrated that $YscU_{CC}$ was able to dissociate from the remaining membrane bound part of YscU *in vivo*.

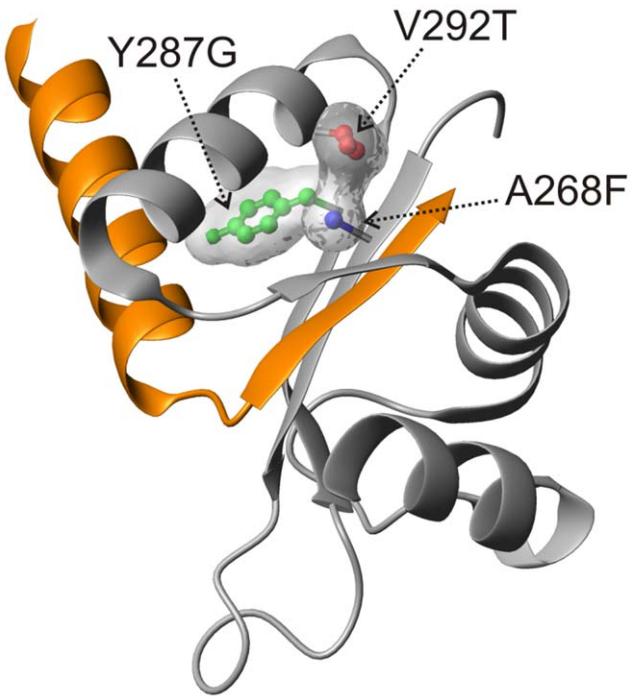

Figure 6. $YscU_C$ suppressor mutations are buried in the structure. The spatial locations of single mutations in $YscU_C$ that suppressed the non-secreting Δ*ysc*P phenotype *in vivo* are shown on the $YscU_C$ structure of *Y. pestis* (2JLI.PDB). All positions are either fully or partially buried in the protein structure. $YscU_{CN}$ and $YscU_{CC}$ polypeptides are colored orange and gray, respectively.
doi:10.1371/journal.pone.0049349.g006

pH-dependencies of $YscU_{CC}$ Dissociation/secretion and Yop Secretion

Unpublished observations from our laboratory indicated that Yop secretion, but not bacterial growth, was influenced by the pH of the growth medium. Further it has been shown that autoproteolysis of $YscU_C$ was pH dependent [15]. Here, we addressed the question of whether dissociation of $YscU_C$ was also pH dependent. First, we subjected cleaved $YscU_C$ to a thermal cycle at pH 6.0 (instead of pH 7.4) by monitoring the thermal signature with CD spectroscopy at 220 nm (Figure 5A). When the resulting thermogram was super-imposed on the thermograms of the wild-type $YscU_C$ at pH 7.4 in presence of 2.5 mM calcium and the non-cleavable mutant P264A in the absence of calcium, they were virtually identical. From this observation, we concluded that $YscU_C$ dissociation was prevented by low pH. $YscU_C$ contains two histidine residues (positions 266 and 324) in the $YscU_{CC}$ fragment that may explain the observed pH-dependency. By monitoring the CD signal at 220 nm as a function of pH, we identified one ionization event in the pH interval of 6.0 to 7.4, with a pKa value of around 6.3 (Figure 5B), and one ionization event around pH 8.0. NMR analyses revealed that both histidines were protonated in response to a pH drop from 7.4 to 6.0 (Figure 5C, 5D). This indicated that the protonation of histidines 266 and 324 was responsible for the observed differences in thermally induced dissociation of $YscU_C$ at pH 6.0 and 7.4. This observation was interesting, because all known YscU orthologs in other T3SSs harbor a conserved histidine residue at the position that corresponds to amino acid 266 in the N ↑ PTH motif. To further dissect the relevance of the two histidines we replaced histidine 324 with alanine (H324A) and studied the *in vitro* response of this mutant to both thermal- and pH perturbations. Since it has been shown that mutation of histidine 266 leads to an *ysc*U mutant affected in autoproteolysis this position is not suitable for an alanine replacement [36]. The H324A variant showed similar dissociation behavior *in vitro* but with reduced thermal stability at pH 7.4 and pH 6.0 compared to wild-type (Figure S3A and S3B).

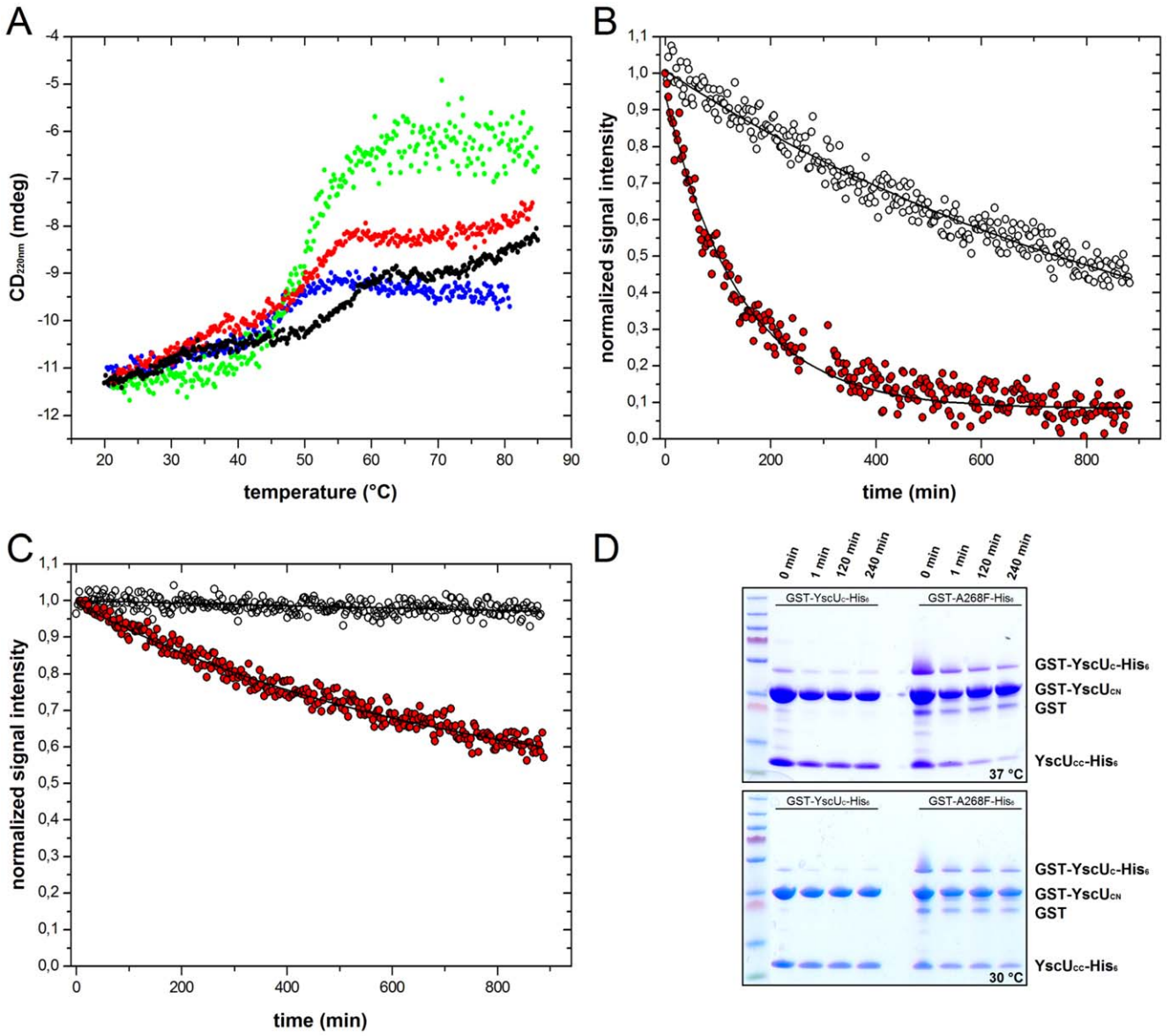

Figure 7. $YscU_C$ suppressor mutant stabilities and dissociation kinetics. (**A**) Thermal induced unfolding of $YscU_C$ and suppressor mutants. Dissociation temperatures (T_{diss}) of single suppressor mutants at pH 7.4 were quantified with the CD signal at 220 nm and a scan rate of 1°C/min; $YscU_C$ (black), A268F (blue), Y287G (green), and V292T (red). All suppressor mutants are destabilized compared to wild-type $YscU_C$. T_{diss} values are summarized in Table 3. (**B**), (**C**) Dissociation kinetics quantified as dissociation life-times (τ_{diss}) of $YscU_C$ (black) and V292T (red) at pH 7.4 followed with NMR-spectroscopy at (B) 37°C and (C) 30°C, respectively. Primary NMR data for (B) is shown in Figure S6. Solid lines correspond to fits of the experimental data to single exponential decays. (**D**) Time dependent GST-pulldown experiments show the dissociation of wild-type $YscU_C$ and the suppressor mutant A268F at 30°C and 37°C after varying incubation times. The suppressor mutant A268F displayed pronounced dissociation of $YscU_{CC}$-His_6 at 37°C and moderate dissociation at 30°C; wild-type $YscU_C$ displayed no dissociation of $YscU_{CC}$-His_6 at 37°C or at 30°C over the observed time period. Note! Dissociation of $YscU_{CC}$ is manifested as disappearance of $YscU_{CC}$-His_6 over time since the dissociation is irreversible and $YscU_{CC}$-His_6 cannot bind itself to the used resin.
doi:10.1371/journal.pone.0049349.g007

The pH-dependency of the CD-signal at 220 nm of the histidine mutant H324A showed a distinct difference compared to the wild-type protein (Figure S3C). Whereas the wild-type protein displayed two ionization events (at pH 6.3 and 8.0) the mutant only displayed the ionization event at pH 6.0. Hence, the pKa of the N↑PTH histidine is around 6, and protonation/deprotonation of this histidine is likely responsible for the difference in thermally induced dissociation at pH 6.0 and 7.4. Next, we wondered whether these biophysical observations reflected biological effects *in vivo*. To investigate the pH-dependency of Yop secretion, we cultivated wild-type *Y. pseudotuberculosis* in Hepes buffered media at pH values between 6.0 and 7.5 in calcium depleted media and monitored the secretion of $YscU_{CC}$ and Yops (Figure 5E and Table 2). Both Yop and $YscU_{CC}$ secretion was maximal at pH levels between 7.0 and 7.5. Secretion gradually decreased when pH was lowered, and at pH 6.0, we observed a pronounced inhibitory effect on the secretion of $YscU_{CC}$ as well as the Yops (albeit not as strong as the inhibition by calcium). Importantly, bacterial growth was not affected by changing the pH of the growth medium; thus, perturbations of external pH values

Table 3. Dissociation temperatures and kinetics of wild-type $YscU_C$ and the suppressor mutants V292T, Y287G, and A268F probed with NMR and CD spectroscopy.

Circular dichroism[a]	T_{diss} (°C)[b]	τ_{diss} at 37°C (min)
$YscU_C$, wild-type	55.2±1.4	stable[c]
V292T	49.5±0.5	60.8±3.2
Y287G	48.9±0.3	138.4±10.5
A268F	44.8±0.5	70.1±4.8
NMR spectroscopy[d]	τ_{diss} at 30°C (min)	τ_{diss} at 37°C (min)
$YscU_C$, wild-type	29914±3526	827±71
V292T	714±47	140±3

CD spectroscopy at 220 nm was performed at a scan rate of 1°C/min to determine the dissociation temperature (T_{diss}) of $YscU_C$ and suppressor mutants (Figure 7A). The kinetics of the dissociation process (τ_{diss}) was monitored with CD spectroscopy at 220 nm and NMR spectroscopy at 37°C and 30°C. See also Figure 7B and 7C; Figure S5B.
[a]measured by following the CD signal at 220 nm;
[b]measured with a scan-rate of 1°C/min;
[c]dissociation was too slow to fit with a single exponential decay function;
[d]measured by following methyl group intensities in one dimensional ^1H spectra.
doi:10.1371/journal.pone.0049349.t003

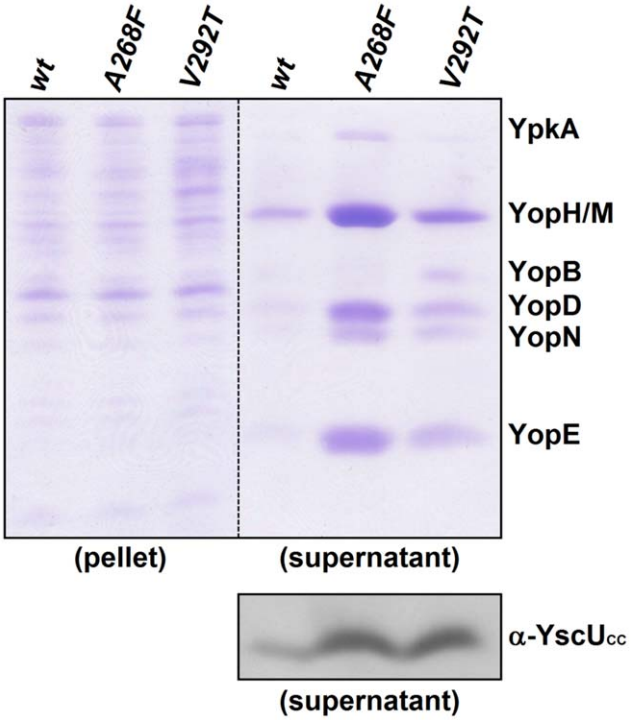

Figure 8. *Yersinia* strains with destabilized *ysc*U suppressor mutants secrete $YscU_{CC}$ and Yops at lower temperatures (30°C) than wild-type. Coomassie stained analysis of Yop secretion in *Y. pseudotuberculosis* incubated at 30°C. Bacteria expressing either wild-type *ysc*U or one of the suppressor mutants, *A268F* or *V292T*. "pellet" indicates intracellular proteins; "supernatant" denotes secreted proteins. Secretion of $YscU_{CC}$ was analyzed on immunoblots with anti-$YscU_{CC}$ peptide antibodies. *Yersinia* harboring *ysc*U suppressor mutants showed strongly elevated secretion of Yops after cultivation at 30°C.
doi:10.1371/journal.pone.0049349.g008

did not cause any general effects on bacterial proliferation (Figure S4). These *in vivo* and *in vitro* results suggested that the pH-dependent secretion of the secretion of Yops and $YscU_{CC}$ was a consequence of the molecular behavior of YscU; i.e., the dissociation and secretion of $YscU_{CC}$ was a prerequisite for maximal secretion of Yop substrates into the culture medium.

Yops are Secreted at Lower Temperatures in Destabilized $YscU_{CC}$ Variants Compared to Wild-type

The results described above suggested that dissociation of $YscU_{CC}$ from the remainder of YscU, followed by secretion of the $YscU_{CC}$ polypeptide, was important for Yop secretion. We and other groups previously showed that single amino acid substitutions in $YscU_C$ could suppress the Yop secretion-deficient phenotype of the *Y. pseudotuberculosis* Δ*ysc*P mutant [17,21,37]. Identification of such suppressor mutations is generally considered as strong genetic evidence for protein-protein interactions. Thus, second-site suppressor mutations are expected to be localized at protein surfaces that are prime positions for protein-protein interactions. In sharp contrast, all amino acid substitutions on the $YscU_{CC}$ polypeptide were either fully or partially buried in the protein structure (Figure 6). Consequently, the underlying mechanism of these mutations must be more complex than a direct protein-protein interaction with YscP. Mutations at buried positions generally act to destabilize proteins; therefore, we reasoned that the altered secretion behavior of the suppressor mutants might be attributed to perturbed stabilities (T_{diss}) and dissociation rates ($k_{diss} = 1/\tau_{diss}$) compared to wild-type $YscU_C$.

To test this notion, we monitored the dissociation kinetics of $YscU_C$ suppressor mutants A268F, Y287G, V292T and wild-type $YscU_C$ with CD and NMR spectroscopy *in vitro*. The resulting dissociation kinetics are reported as dissociation lifetimes (τ_{diss}), or the reciprocal of the dissociation rate ($= 1/k_{diss}$). Because Yop secretion is triggered by a temperature shift from 26°C to 37°C [3,4,6], we initially performed the assays at 37°C. We found that all $YscU_C$ mutants were folded (Figure S5A) and displayed decreased thermal stabilities compared to wild-type $YscU_C$, evident from the reduced dissociation temperatures (Figure 7A and Table 3). We quantified the dissociation kinetics with both CD and NMR spectroscopy for the $YscU_C$ variant V292T; with CD, we detected changes in ellipticity at 220 nm that accompanied dissociation (Figure S5B); with NMR, we detected the loss of resonance intensities for residues in the $YscU_{CC}$ fragment (Figure S6). The time-dependent signals were well described by first order processes; accordingly, all kinetic traces could be fit accurately with single exponential decay functions. Both CD and NMR results indicated that wild-type $YscU_C$ displayed very slow dissociation kinetics at 37°C in the observed time frame; in comparison, the $YscU_C$ variant V292T displayed a significantly enhanced rate of dissociation (Figure 7B, Figure S6A, S6B). It should be noted that the observed variations in the dissociation lifetimes (τ_{diss}) for the suppressor mutants are dependent on the method used for quantification (Table 3). For instance, τ_{diss} for the V292T variant was 61 min and 140 min, based on CD and NMR, respectively. This discrepancy could be attributed to differences in sensitivity; the CD signal was directly sensitive to the dissociation process, but NMR required both dissociation and aggregation for a reduction in signal intensity. Hence, both dissociation and aggregation were slow processes that occurred at similar time scales *in vitro*. After one hour at 37°C, a significant fraction of the V292T variant displayed dissociated species (65% and 38% from CD and NMR, respectively), but wild-type $YscU_C$ remained intact under the same conditions.

V292T displayed a significantly reduced thermal stability compared to wild-type $YscU_C$; therefore, we also performed

NMR-based kinetic experiments at 30°C (Figure 7C). At this temperature, wild-type $YscU_C$ was stable over the entire experiment (860 min), but the V292T variant dissociated at a rate equal to the rate for wild-type $YscU_C$ at 37°C, within experimental error (Table 3). We confirmed these results with the A268F suppressor mutant. Further we used a GST pull down assay, and the dissociation of GST-$YscU_C$-His_6 respectively GST-A268F-His_6 was monitored at 30°C and 37°C. Indeed, GST-$YscU_C$-His_6 was completely stable at both temperatures, but GST-A268F-His_6 dissociated to a significant extent over time, visible in the decrease of the $YscU_{CC}$-His_6 content at both 30°C and 37°C (Figure 7D).

Because the dissociation of $YscU_C$ is required for Yop secretion *in vivo*, we expected suppressor mutant strains to secrete Yops at lower temperatures compared to the wild-type strain. To test this hypothesis, we probed for the presence of secreted Yops and $YscU_{CC}$ in the culture supernatant in strains that carried either *ysc*U or *ysc*U suppressor mutants *A268F* or *V292T* after a temperature shift from 26°C to 30°C. Both the *A268F* and *V292T* mutant strain secreted Yops and $YscU_{CC}$ already at 30°C; in contrast, the wild-type strain showed almost no secretion at this temperature (Figure 8). Probing for LcrV and YscI as early substrates in T3SS confirmed the direct link between secretion of $YscU_{CC}$ and T3SS substrates (Figure S7B). Despite the increased secretion of Yops at reduced temperatures, the pH regulation was still active in these *Yersinia* mutants. *A268F* and *V292T* revealed the same secretion pattern like the wild-type when grown in media with different pH (Figure 5E and Figure S7A). Importantly, all strains secreted Yops in a calcium-regulated manner; this showed that the suppressor mutants retained calcium sensing capability (data not shown).

Our results showed a strong link between *in vivo* and *in vitro* results for dissociation of the $YscU_{CC}$ polypeptide from the remainder of the protein. This demonstrated that not only autoproteolytic cleavage but also dissociation and secretion of $YscU_{CC}$ is a key step in the regulation of Yop secretion.

Discussion

The YscU protein of *Yersinia pseudotuberculosis* and orthologs in other bacteria display autoproteolytic activity, with cleavage at a conserved N ↑ PTH motif. It is reasonable to assume that a strictly conserved autoproteolytic activity in a protein is linked to a specific function in the organism. Auto-processing has been observed in other proteins; e.g., in the SEA domain of the membrane-bound MUC1 protein, the processing occurs at a conserved GD ↑ PH site. It has been suggested that this cleavage introduces a molecular-mechanical fracture that protects epithelial cells from rupture [38]. It was previously postulated that autoproteolysis of YscU exposes a new binding surface to other T3SS proteins by changing the charge distribution at the cleavage site [39]. Here, we propose an alternative model, where dissociation of $YscU_{CC}$ from the membrane anchored segment of YscU, followed by $YscU_{CC}$ secretion via the T3SS, plays a central role in the substrate specificity switch [21].

We showed that T3SS mediated Yop secretion correlated with the secretion of $YscU_{CC}$ and presumed a fully functional T3SS. Secretion of $YscU_{CC}$ required autocatalytic cleavage of the cytosolic domain ($YscU_C$) of the inner membrane protein YscU that was linked in earlier studies to be one key regulator in the substrate specificity switch of T3SS mediated Yop secretion [17]. *In vitro* analysis with recombinantly produced $YscU_C$ confirmed the dissociation capacity of the protein and revealed potential regulating factors, like divalent ions (i.e. calcium), pH and temperature. We showed that T3SS mediated Yop secretion was strongly affected by 0.5 to 1 mM calcium and pH values below 6.5. The calcium concentration had an "all or nothing" effect on Yop secretion. In contrast, the inhibitory effect of low pH values was less pronounced. Surprisingly Ca^{2+}-ions bound to $YscU_C$ with a K_d of 800 μM *in vitro*; notably, this value was consistent with the threshold value for calcium dependent down-regulation of Yop secretion *in vivo*. Additional *in vitro* analysis including different divalent cations Mg^{2+}, Sr^{2+} and Ba^{2+} indicated that the alkaline earth metal ions interacted and stabilized $YscU_{CC}$ binding to about the same extent. These results indicated that the calcium regulation of the *Yersinia* T3SS *in vivo* is complex and cannot be explained only on basis of the $YscU_C$ calcium interaction. The N ↑ PTH histidine, is unfortunately not suitable for mutations to other amino acids since it affects the autoproteolytic activity [36]. However experiments where histidine 324 was replaced with alanine indicated that, overall, the N ↑ PTH histidine is responsible for the pH-dependency of $YscU_C$ dissociation. Thus these findings suggest that pH is also an extracellular queue regulating the *Yersinia* T3SS.

It is known that the YscP protein plays an important role in the regulation of the substrate specificity switch [17]. We recently proposed that YscP activity may stimulate displacement of $YscU_{CC}$ from the remaining YscU part, and that this activity was triggered by target cell contact or calcium depletion. We further suggested that, in *ysc*U suppressor mutants, the point mutations in $YscU_{CC}$ induced a perturbation in the YscU structure, which destabilized the interaction between $YscU_{CC}$ and the remaining membrane anchored part of YscU [16]. This was suggested because the whole *ysc*P gene was deleted; thus, it was likely that the $YscU_{CC}$ mutations caused a gain of function. In the present study, we confirmed this hypothesis by showing that destabilization of the suppressor mutants led to premature $YscU_{CC}$ dissociation, which then induced Yop secretion. Strains that carried the suppressor mutations secreted Yops at 30°C in calcium-depleted medium. This finding contrasted with findings in the wild-type strain, which showed almost no Yop secretion at 30°C. Nevertheless, all suppressor mutants retained the wild-type calcium regulation of Yop secretion indicating that calcium exhibits a stabilizing effect on the interaction between $YscU_{CC}$ and the remainder of YscU.

Surprisingly, we found that $YscU_{CC}$ was also secreted via the T3SS; this was remarkable, given that YscU is an inner membrane protein [40]. Our results favor a model where YscU orchestrates obstruction of the T3SS secretion channel. This block is thus, relieved through $YscU_{CC}$ secretion in calcium depleted and in pH ≥6.5 conditions. In support for this model is the observation that *ysc*U mutants impeded for autoproteolysis and subsequent secretion of $YscU_{CC}$ (mutations within the NPTH motif) are unable to secrete the Yop-proteins [18]. Further, these mutants secrete elevated amounts of the early substrate YscF showing that the T3SS is active in these mutants and allows secretion of early but not late substrates [16]. The model explains why these mutants are also defective in Yop secretion. Further support for this model was our finding that the "Ca^{2+}-blind" *yop*N mutant, unable to respond to extracellular calcium, secreted $YscU_{CC}$ as well as Yops in Ca^{2+} containing conditions indicating that $YscU_{CC}$ secretion is tightly coupled to Yop secretion. Thus, YopN is essential for the calcium response in *Yersinia* and in addition our results suggest that YopN has a role in the Ca^{2+} response *in vivo* leading to stabilization of YscU. Moreover, Mg^{2+} blocks $YscU_{CC}$ displacement *in vitro* similarly to Ca^{2+} but in contrast the pathogen secretes Yops *in vivo* at high concentrations of Mg^{2+}, indicating that Mg^{2+} is not interacting with $YscU_C$ during *in vivo* conditions. Thus it is

possible that YopN discriminates between the ions, allowing transport/uptake of Ca^{2+} but not Mg^{2+} during growth at 37°C *in vivo*. YopN has also been shown to be surface located when *Yersinia* is grown at 37°C in presence of calcium which agrees with its putative role as calcium scavenger [35].

This study has provided a new handle for investigating the function of YscU/FlhB proteins in other bacteria. Given the conservation within this family of proteins, it is likely that they also exhibit regulatory roles that involve secretion of the processed C-terminus of the protein. However, depending on life style, the actual triggering signal may differ among different pathogens. For example, *Salmonella* invasion is controlled by environmental pH, low oxygen, and acetate [41]. Although different intracellular regulatory pathways have been linked to these signals, virtually nothing is known about signal reception and interpretation by the pathogen. Based on the results presented here, it would not be surprising to find that some signals stimulated secretion of the *Salmonella* $YscU_{CC}$ homolog, $SpaS_{CC}$.

Supporting Information

Figure S1 Reversibility of the high temperature (77°C) transition of $YscU_C$. Thermal up- and down-scans of 10 μM $YscU_C$ were monitored with CD spectroscopy at 220 nm. $YscU_C$ was subjected to two sequential thermal cycles (one cycle: 20°C to 95°C and then back to 20°C). The color coding indicates: first up-scan (black), first down-scan (open gray), second up-scan (open blue) and second down-scan (open red). After initial loss of secondary structure, the high temperature transition is reversible.
(TIF)

Figure S2 Calcium induced chemical shift perturbations in $YscU_C$. (**A**) Chemical shift differences were monitored with two-dimensional ^1H-^{15}N HSQC NMR spectra of $YscU_C$ before and after saturation with calcium. Chemical shift differences are plotted against the primary sequence. The blue line indicates the threshold value (0.06 ppm) used in (B) to highlight amino acid residues affected by addition of calcium. Residues responding to calcium are confined to the $YscU_{CC}$ fragment. (**B**) Structural distributions of residues that show significant chemical shift perturbations in response to calcium binding are shown in red on the $YscU_C$ structure (2JLI.PDB). $YscU_{CN}$ and $YscU_{CC}$ fragments are colored orange and gray, respectively.
(TIF)

Figure S3 Biophysical analysis of the $YscU_C$ variant H324A. (**A**) Thermal up- and down-scans of H324A at pH 7.4 monitored with CD spectroscopy at 220 nm in the absence of calcium. (**B**) Thermal up- and down-scans of H324A at pH 6.0 monitored with CD spectroscopy at 220 nm in the absence of calcium. Up- and down scans of H324A are shown in red and blue circles, respectively. (**C**) The pH-dependency of the CD-signal at 220 nm for H324A.
(TIF)

Figure S4 *Y. pseudotuberculosis* growth kinetics were pH independent between pH 6.0 and pH 7.5. Bacterial growth of wild-type *Y. pseudotuberculosis* was analyzed by monitoring the optical density (OD_{600}) under (**A**) calcium-supplemented and (**B**) calcium-depleted conditions. Bacteria were cultivated 2 h at 26°C, then 3 h at 37°C. Samples were taken every hour to monitor the growth based on the measured OD_{600}. No significant differences in growth kinetics were observed within the monitored pH-interval of 6.0 to 7.5.
(TIF)

Figure S5 Secondary structure analysis and dissociation kinetics of $YscU_C$ suppressor mutants monitored with CD spectroscopy. (**A**) Far-UV CD spectra of 10 μM wild-type $YscU_C$ (black) and the suppressor mutants A268F (blue), Y287G (green), V292T (red). The similarity in the shape of the CD signals indicates that all $YscU_C$ variants have similar secondary structure. (**B**) Dissociation kinetics of $YscU_C$ (black) and suppressor mutants A268F (blue), Y287G (green), and V292T (red) were monitored with CD spectroscopy at 220 nm and 37°C. The solid lines represent the best fit of a single exponential decay function to determine τ_{diss}. Dissociation kinetics are summarized in Table 3. Note that the data points at time = zero have been normalized for clarity.
(TIF)

Figure S6 Primary NMR data used to quantify dissociation kinetics of wild-type $YscU_C$ and V292T at 37°C. Shown are expansions of methyl resonances from one-dimensional ^1H spectra at various time points for (**A**) wild-type $YscU_C$ and (**B**) the V292T mutant (see Figure 7B and 7C).
(TIF)

Figure S7 Secretion analysis of *yscU* suppressor mutants *A268F* and *V292T*. (**A**) Secretion analysis of *A268F* and *V292T* after cultivation in Hepes-buffered LB at different pH values. Yop secretion was induced by calcium depletion and a temperature shift from 26°C to 37°C. *A268F* and *V292T* showed elevated Yop secretion at pH≥6.5 and strong inhibition at pH 6.0 (**B**) Secretion analysis of *A268F* and *V292T* at pH 7.5 and 30°C compared to wild-type. The T3SS was induced by calcium depletion and a temperature shift to 30°C. *A268F* and *V292T* showed a strongly elevation of Yop secretion. Coomassie stained gels demonstrate secreted Yops. "pellet" indicates intracellular proteins; "supernatant" denotes secreted proteins. The secretion of YscI and LcrV was visualized on immunoblots with anti-YscI and anti-LcrV antibodies.
(TIF)

Figure S8 Size exclusion chromatography-based estimation of the $YscU_{CC}$ aggregate size. Chromatogram of analytical size exclusion chromatography of purified $YscU_{CC}$. $YscU_{CC}$ eluted in the void volume of the SEC column.
(TIF)

Figure S9 CD-based analysis of $YscU_{CC}$ produced by thermal stimulation or by recombinant protein production. Comparison of $YscU_C$ CD spectra at 20°C after one completed thermal cycle to 95°C. Filled circles show the $YscU_{CC}$ produced by thermal stimulation and open circles show the purified $YscU_{CC}$ fragment, produced *in vitro* by recombinant protein production. The similarity of the spectra shows that the residual CD signal of $YscU_C$ after one thermal cycle is dominated by the $YscU_{CC}$ fragment.
(TIF)

Table S1 Bacterial strains and plasmids used in this study.
(RTF)

Table S2 Primers used in this study.
(RTF)

Materials and Methods S1 Procedure for cloning *yscU*$_{CC}$ into pBADmyc His B.
(RTF)

Materials and Methods S2 Cloning procedure for GST fusion proteins.
(RTF)

Results S1 $YscU_{CC}$ aggregated after dissociation from $YscU_{CN}$. Analytical size exclusion chromatography was used to show that $YscU_{CC}$ aggregates after dissociation from the $YscU_{CN}$ polypeptide.
(RTF)

Results S2 Persistent secondary structure in aggregated $YscU_{CC}$ from CD spectroscopy. CD spectroscopy on thermally and recombinantly produced $YscU_{CC}$ aggregates was used to show that $YscU_{CC}$ contains elements of secondary structure in the aggregated state.
(RTF)

References

1. Hills GM, Spurr ED (1952) The effect of temperature on the nutritional requirements of Pasteurella pestis. J Gen Microbiol 6: 64–73.
2. Higuchi K, Kupferberg LL, Smith JL (1959) Studies on the nutrition and physiology of Pasteurella pestis. III. Effects of calcium ions on the growth of virulent and avirulent strains of Pasteurella pestis. J Bacteriol 77: 317–321.
3. Bölin I, Portnoy DA, Wolf-Watz H (1985) Expression of the temperature-inducible outer membrane proteins of yersiniae. Infect Immun 48: 234–240.
4. Heesemann J, Algermissen B, Laufs R (1984) Genetically manipulated virulence of Yersinia enterocolitica. Infect Immun 46: 105–110.
5. Portnoy DA, Falkow S (1981) Virulence-associated plasmids from Yersinia enterocolitica and Yersinia pestis. J Bacteriol 148: 877–883.
6. Portnoy DA, Wolf-Watz H, Bölin I, Beeder AB, Falkow S (1984) Characterization of common virulence plasmids in Yersinia species and their role in the expression of outer membrane proteins. Infect Immun 43: 108–114.
7. Cornelis GR, Van Gijsegem F (2000) Assembly and function of type III secretory systems. Ann Rev Microbiol 54: 735–774.
8. Galan JE, Wolf-Watz H (2006) Protein delivery into eukaryotic cells by type III secretion machines. Nature 444: 567–573.
9. Marlovits TC, Kubori T, Lara-Tejero M, Thomas D, Unger VM, et al. (2006) Assembly of the inner rod determines needle length in the type III secretion injectisome. Nature 441: 637–640.
10. Akopyan K, Edgren T, Wang-Edgren H, Rosqvist R, Fahlgren A, et al. (2011) Translocation of surface-localized effectors in type III secretion. Proc Natl Acad Sci U S A 108: 1639–1644.
11. Cornelis GR, Wolf-Watz H (1997) The Yersinia Yop virulon: a bacterial system for subverting eukaryotic cells. Mol Micro 23: 861–867.
12. Pettersson J, Nordfelth R, Dubinina E, Bergman T, Gustafsson M, et al. (1996) Modulation of virulence factor expression by pathogen target cell contact. Science 273: 1231–1233.
13. Rosqvist R, Magnusson KE, Wolf-Watz H (1994) Target cell contact triggers expression and polarized transfer of Yersinia YopE cytotoxin into mammalian cells. EMBO J 13: 964–972.
14. Michiels T, Wattiau P, Brasseur R, Ruysschaert JM, Cornelis G (1990) Secretion of Yop Proteins by Yersiniae. Infect and Immun 58: 2840–2849.
15. Ferris HU, Furukawa Y, Minamino T, Kroetz MB, Kihara M, et al. (2005) FlhB regulates ordered export of flagellar components via autocleavage mechanism. J Biol Chem 280: 41236–41242.
16. Björnfot AC, Lavander M, Forsberg A, Wolf-Watz H (2009) Autoproteolysis of YscU of Yersinia pseudotuberculosis is important for regulation of expression and secretion of Yop proteins. J Bacteriol 191: 4259–4267.
17. Edqvist PJ, Olsson J, Lavander M, Sundberg L, Forsberg A, et al. (2003) YscP and YscU regulate substrate specificity of the Yersinia type III secretion system. J Bacteriol 185: 2259–2266.
18. Lavander M, Sundberg L, Edqvist PJ, Lloyd SA, Wolf-Watz H, et al. (2002) Proteolytic cleavage of the FlhB homologue YscU of Yersinia pseudotuberculosis is essential for bacterial survival but not for type III secretion. J Bacteriol 184: 4500–4509.
19. Lavander M, Sundberg L, Edqvist PJ, Lloyd SA, Wolf-Watz H, et al. (2003) Characterisation of the type III secretion protein YscU in Yersinia pseudotuberculosis. YscU cleavage-dispensable for TTSS but essential for survival. Adv Exp Med Biol 529: 109–112.
20. Minamino T, Macnab RM (2000) Domain structure of Salmonella FlhB, a flagellar export component responsible for substrate specificity switching. J Bacteriol 182: 4906–4914.
21. Williams AW, Yamaguchi S, Togashi F, Aizawa S, Kawagishi I, et al. (1996) Mutations in fliK and flhB affecting flagellar hook and filament assembly in Salmonella typhimurium. J Bacteriol 178: 2960–2970.
22. Sorg I, Wagner S, Amstutz M, Müller SA, Broz P, et al. (2007) YscU recognizes translocators as export substrates of the Yersinia injectisome. EMBO J 26: 3015–24.
23. Agrain C, Callebaut I, Journet L, Sorg I, Paroz C, et al. (2005) Characterization of a Type III secretion substrate specificity switch (T3S4) domain in YscP from Yersinia enterocolitica. Mol Micro 56: 54–67.
24. Morris DP, Roush ED, Thompson JW, Moseley MA, Murphy JW, et al. (2010) Kinetic characterization of Salmonella FliK-FlhB interactions demonstrates complexity of the Type III secretion substrate-specificity switch. Biochem 49: 6386–6393.
25. Kubori T, Sukhan A, Aizawa SI, Galan JE (2000) Molecular characterization and assembly of the needle complex of the Salmonella typhimurium type III protein secretion system. Proc Natl Acad Sci U S A 97: 10225–10230.
26. Botteaux A, Sani M, Kayath CA, Boekema EJ, Allaoui A (2008) Spa32 interaction with the inner-membrane Spa40 component of the type III secretion system of Shigella flexneri is required for the control of the needle length by a molecular tape measure mechanism. Mol Micro 70: 1515–1528.
27. Tamano K, Katayama E, Toyotome T, Sasakawa C (2002) Shigella Spa32 is an essential secretory protein for functional type III secretion machinery and uniformity of its needle length. J Bacteriol 184: 1244–1252.
28. Grzesiek S, Bax A (1992) Improved 3D triple-resonance NMR techniques applied to a 31-Kda protein. J Magn Reson 96: 432–440.
29. Wittekind M, Mueller L (1993) HNCACB, a high-sensitivity 3D NMR experiment to correlate amide-proton and nitrogen resonances with the alpha-carbon and beta-carbon resonances in proteins. J Magn Res Series B 101: 201–205.
30. Delaglio F, Grzesiek S, Vuister GW, Zhu G, Pfeifer J, et al. (1995) NMRPipe: a multidimensional spectral processing system based on UNIX pipes. J Biomol NMR 6: 277–293.
31. Helgstrand M, Kraulis P, Allard P, Härd T (2000) Ansig for Windows: an interactive computer program for semiautomatic assignment of protein NMR spectra. J Biomol NMR 18: 329–336.
32. Consalvi V, Chiaraluce R, Giangiacomo L, Scandurra R, Christova P, et al. (2000) Thermal unfolding and conformational stability of the recombinant domain II of glutamate dehydrogenase from the hyperthermophile Thermotoga maritima. Protein Eng 13: 501–507.
33. van Holde KE, Johnson WC, Ho PS (1998) Physical biochemistry. Prentice-Hall, Inc Simon & Schuster.
34. Zahorchak RJ, Charnetzky WT, Little RV, Brubaker RR (1979) Consequences of Ca2+ deficiency on macromolecular synthesis and adenylate energy charge in Yersinia pestis. J Bacteriol 139(3): 792.
35. Forsberg A, Viitanen AM, Skurnik M, Wolf-Watz H (1991) The surface-located YopN protein is involved in calcium signal transduction in Yersinia pseudotuberculosis. Mol Microbiol 5(4): 977–86.
36. Wiesand U, Sorg I, Amstutz M, Wagner S, van den Heuvel J, et al. (2009) Structure of the type III secretion recognition protein YscU from Yersinia enterocolitica. J Mol Biol 385(3): 854–66.
37. Kutsukake K, Minamino T, Yokoseki T (1994) Isolation and characterization of FliK-independent flagellation mutants from Salmonella typhimurium. J Bacteriol 176: 7625–7629.
38. Macao B, Johansson DG, Hansson GC, Härd T (2006) Autoproteolysis coupled to protein folding in the SEA domain of the membrane-bound MUC1 mucin. Nat Struct Mol Biol 13: 71–76.
39. Lountos GT, Austin BP, Nallamsetty S, Waugh DS (2009) Atomic resolution structure of the cytoplasmic domain of Yersinia pestis YscU, a regulatory switch involved in type III secretion. Protein Sci 18: 467–474.
40. Allaoui A, Woestyn S, Sluiters C, Cornelis GR (1994) YscU, a Yersinia-Enterocolitica Inner Membrane-Protein Involved in Yop Secretion. J Bacteriol 176: 4534–4542.
41. Durant JA, Corrier DE, Ricke SC (2000) Short-chain volatile fatty acids modulate the expression of the hilA and invF genes of Salmonella Typhimurium. J Food Protect 63: 573–578.

Acknowledgments

We thank Glenn Björk, Åke Forsberg and Pernilla Wittung-Stafshede for discussion and valuable criticism; we thank Software Scientifics Sweden AB for providing Figure Adapter® to aid in figure management and we acknowledge the Umeå Protein Expertise Platform where parts of the work have been done.

Author Contributions

Conceived and designed the experiments: SF HWW MWW. Performed the experiments: SF OH CFW FHL. Analyzed the data: SF OH CFW FHL. Wrote the paper: SF HWW MWW.